J Mol Model (2013) 19:3843–3850
DOI 10.1007/s00894-013-1922-9

ORIGINAL PAPER

A DFT study on the sensing behavior of a BC_2N nanotube toward formaldehyde

Maziar Noei · Ali Ahmadi Peyghan

Received: 8 February 2013 / Accepted: 12 June 2013 / Published online: 26 June 2013

Abstract We investigated the viability of using a BC_2N nanotube to detect formaldehyde (H_2CO) molecule by means of B3LYP and M06 density functionals. The results indicate that the molecule is weakly adsorbed on the intrinsic BC_2N nanotube releasing energy of 0.8 kcal mol^{-1} (at B3LYP/6-31G(d)) without significant effect on the HOMO-LUMO energy gap and electrical conductivity of the tube. Thus, H_2CO cannot be detected using this intrinsic nanotube. To overcome this problem, a carbon atom of the tube wall was substituted by a Si atom. It was demonstrated that the Si-doped tube cannot only strongly adsorb the H_2CO molecule, but also may effectively detect its presence because of the increase in the electric conductivity of the tube.

Keywords Band gap · B3LYP · DFT · Nanostructures · Sensor

Introduction

Carbon nanotubes (CNTs) are very prevalent in today's world of research and their unique properties have prompted interest to produce inorganic nanomaterials [1–7]. The similarity between graphite and the hexagonal boron nitride (h-BN) leads to the production of boron nitride nanotubes (BNNTs). Contrary to CNTs, the electronic properties of BNNTs are almost independent of the tube chirality and its diameter. The BNNTs present partial ionic B-N bonds and form a slight buckling on the surface that may be helpful for the adsorption of molecules which interact weakly with CNT surfaces. Another important difference resides in the fact that while CNTs are easily oxidized, BNNTs present strong resistance to oxidation [8]. Similar to h-BN, the mixed $B_xC_yN_z$ compounds (x, y, and z indicate the stoichiometry) are stable in the hexagonal structure and they were predicted to form one- and two-dimensional nanostructures [9–11]. The BC_2N stoichiometry is believed to be one of the most stable forms of the ternary BCN layers and nanotubes [12]. Considerable experimental efforts have been devoted to the synthesis of $B_xC_yN_z$ nanotubes, and they have been successfully obtained by electrical pyrolysis, laser ablation, hot-filament chemical vapor deposition, and the template route [13–16].

As an important industrial chemical, formaldehyde (H_2CO) is utilized in the manufacturing of building boards, plywood, and lacquer materials [17, 18]. Moreover, it is an intermediate in consumer products, such as detergents and soaps, and also it is used in pharmacology and medicine because of its sterilization property. It is known that formaldehyde gas can cause asthma-like symptom and induce central nervous system and immune system damage, as well as blindness and respiratory disease [19, 20]. The maximum legal levels in dwellings and work places are limited in most countries. The formaldehyde vapors can cause various effects to human health on the basis of the air concentration. Therefore, effective methods to monitor formaldehyde have been demanded for atmospheric and environmental measurement and control. People have been looking for good materials as gas sensors with high sensitivity for a long time. Basically, it is expected that the adsorption of gas molecules on the sensors is stable and the changes of the conductivity should be observable. However, most of gases are found physisorbed on suspended intrinsic nanotubes [21–23]. On the contrary, the dopants and defects in nanotubes can strongly enhance the adsorption of molecules [24, 25], indicating that doped atoms and defects play important roles in the applications of them. In the present work, within the density functional theory (DFT) framework, the interaction of H_2CO with BC_2NNTs will be investigated based on analyses of structure, energies, electronic properties, etc. We are interested

M. Noei
Department of Chemistry, Mahshahr Branch, Islamic Azad University, Mahshahr, Iran

A. A. Peyghan (✉)
Central Tehran Branch, Islamic Azad University, Tehran, Iran
e-mail: ahmadi.iau@gmail.com

in whether there is a possibility of BC_2NNTs serving as chemical sensors for detecting H_2CO molecule, and if not, can we find a method for improving the sensitivity of BC_2NNTs to H_2CO?

Computational methods

Geometry optimizations, natural bond order (NBO) analysis, and density of states (DOS) analysis were performed on a (8, 0) zigzag BC_2NNT (constructed of 24 B, 24 N and 48 C atoms), and different H_2CO/BC_2NNT complexes by using B3 (Becke three parameter exchange functional [26] and the correlation functional of Lee, Yang and Parr (LYP) [27]) with 6-31G(d) basis set as implemented in GAMESS suite of program [28]. Default convergence tolerances were used. B3LYP is a popular functional which has been commonly used for nanostructures [29–32]. The length and the diameter of the optimized pure BC_2NNT were computed to be about 11.42 Å and 6.22 Å, respectively. In order to reduce the boundary effects, atoms at the open ends of the tube were saturated with hydrogen atoms. The adsorption energy (E_{ad}) of a HCN molecule on the tube is obtained using the following equation:

$$E_{ad} = E\left(\text{tube}/H_2CO\right) - E(\text{tube}) - E(H_2CO) + E_{BSSE} \quad (1)$$

where E (tube/H_2CO) is the total electronic energy of mentioned molecule adsorbed on the BC_2NNT surface, and E (tube) and E (H_2CO) are the total electronic energies of the tube and a molecule, respectively. E_{BSSE} is the basis set superposition error (BSSE) corrected for the all interaction energies. The BSSE was obtained using counterpoise method [33]. By the definition, a negative value of E_{ad} corresponds to exothermic adsorption. The canonical assumption for Fermi level (E_F) is that in a molecule (at T=0 K) it lies approximately in the middle of the highest occupied molecular orbital (HOMO) and the lowest unoccupied molecular orbital (LUMO) energy gap (E_g). It is noteworthy to mention that, in fact, what lies in the middle of the E_g is the chemical potential, and since the chemical potential of a free gas of electrons is equal to its Fermi level as traditionally defined, herein, the Fermi level of the considered systems is at the center of the E_g.

Results and discussion

H_2CO adsorption on pristine BC_2NNT

At first, the accuracy of the method used in this work has been tested initially to describe the properties of H_2CO molecule. The bond length of individual C-H and bond angle of H-C-H in free H_2CO are about 1.11 Å and 115º, which are in good agreement with the experimental values of 1.01 Å and 118º [34], respectively. In Fig. 1, we have shown the side view of the optimized structure (partial) of the BC_2NNT, where four types of bonds, namely B-N, B-C, N-C and C-C, can be identified with corresponding lengths of 1.46, 1.52, 1.44 and 1.36 Å, respectively. There are two types of carbon atoms in the BC_2NNT; C_1 is a carbon atom that is bonded to two B atoms and one C atom, while C_2 is a carbon atom that is bonded to two N atoms and one C atom. In the C–C bonds, the C_1 atoms are relaxed outward while the C_2 atom is relaxed inward of the tube surface.

In order to obtain stable configurations (local minima) of single H_2CO adsorbed on the BC_2NNT, various possible initial adsorption geometries including single (hydrogen, carbon or oxygen), double (H–C or C–O) and triple (H–C–H or H–C–O) bonded atoms close to B, N, C_1 and C_2 atoms are considered. However, only one local minimum structure was obtained after

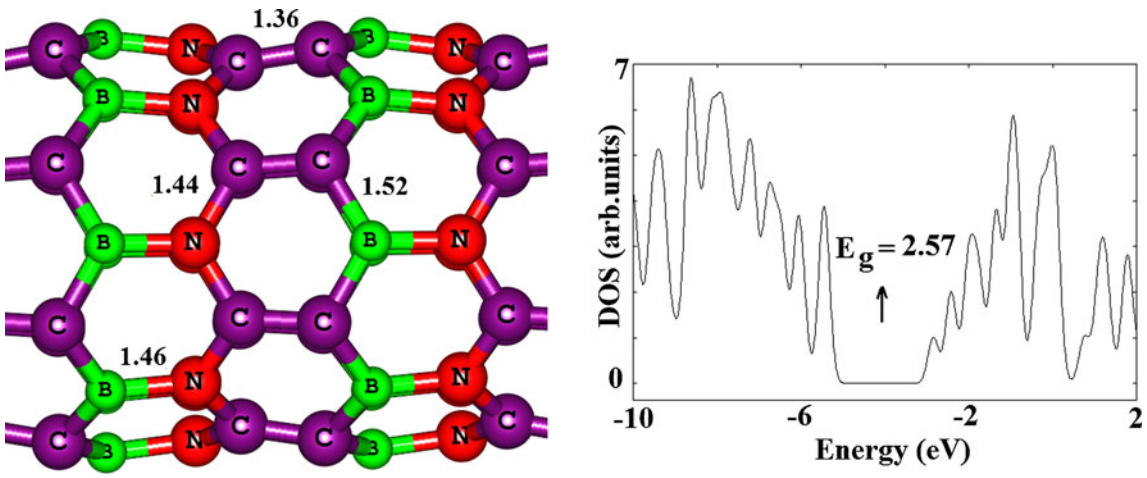

Fig. 1 Optimized structure (partial) of BC_2NNT and its density of states (DOS). Distances are in Å

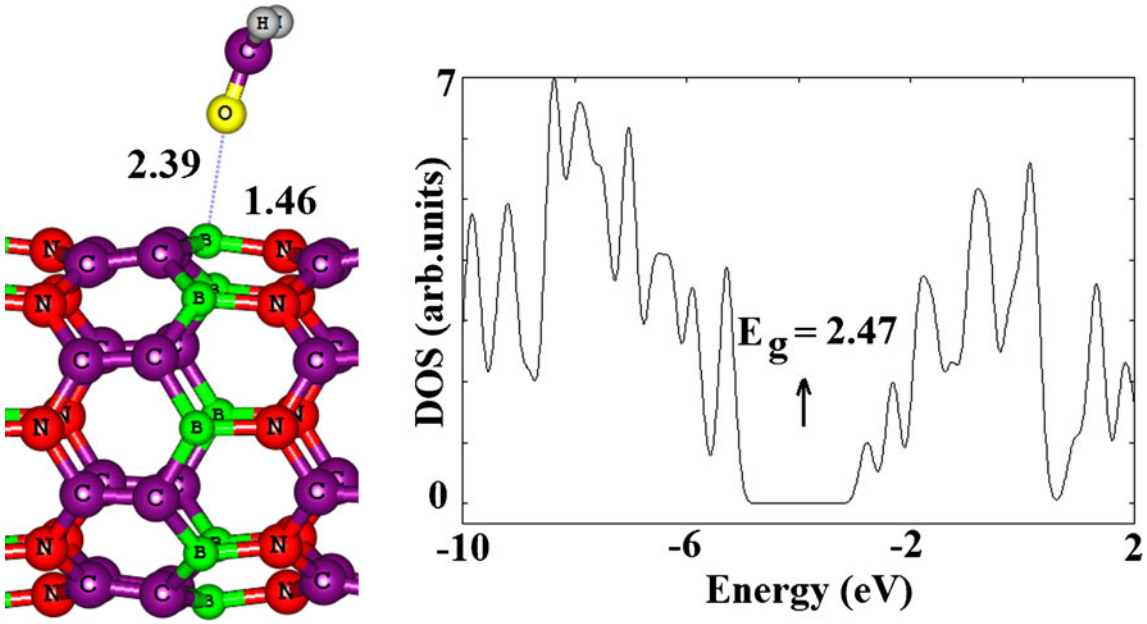

Fig. 2 Model for stable adsorption state for a H_2CO molecule on the pristine BC_2NNT and its density of states (DOS) plots. Distances are in Å

the relaxation process (Fig. 2). In this configuration, H_2CO molecule was located on the top of a boron atom of the tube wall from its oxygen head and the corresponding calculated E_{ad} value is about −0.8 kcal mol^{-1}. The less negative E_{ad} of H_2CO on pristine BC_2NNT in this structure reveals the physical nature of the interaction. The interaction distances of B…O is about 2.39 Å and a small Mulliken charge of 0.043 *e* is transferred from the molecule to the tube (Table 1). It is worth saying that other initial configurations re-oriented to this stable configuration.

To investigate the effect of adsorption process on the electronic properties of pristine BC_2NNT, the DOS plots were calculated for the tube and H_2CO/tube complex. For the bare BC_2NNT (Fig. 1), it can be concluded that it is a semiconducting material with an E_g of 2.57 eV. By referring to Fig. 2, both conduction and valence levels slightly move to higher energies, so that E_g of the tube increased from 2.57 eV in bare tube to 2.47 eV for H_2CO/BC_2NNT complex because of charge transfer to the tube. This change in electronic property is negligible indicating that BC_2NNT is still a semiconductor after H_2CO adsorption. Thus, we conjecture that the electronic properties of pristine BC_2NNT are insensitive to the H_2CO molecule.

Similar to results of Zhang et al. [35] about pristine BNNT, the electronic properties of BC_2NNT are insensitive to H_2CO molecules. Unlike BC_2NNTs and BNNTs, conductivity of pristine SiC nanotubes (SiCNTs) is affected by formaldehyde, so that with increasing the coverage of H_2CO molecules, the band gap of SiCNT is gradually decreased, thereby increasing its conductivity. It is expected that SiCNT could be a promising gas sensor for H_2CO molecule [36].

Table 1 Calculated adsorption energy of a H_2CO (E_{ad}, kcal mol^{-1}), HOMO energies (E_{HOMO}), LUMO energies (E_{LUMO}), Fermi level energies and HOMO-LUMO energy gap (E_g) for pristine and Si doped BC_2NNT at B3LYP/6-31G(d). Energies are in eV

System	E_{ad}	[a]Q_T (e)	E_{HOMO}	E_F	E_{LUMO}	E_g	[b]ΔE_g(%)
BC_2NNT	–	–	−5.41	−4.12	−2.84	2.57	–
H_2CO/BC_2NNT	−0.8	0.043	−5.24	−4.00	−2.77	2.47	−3.9
Si_1-BC_2NNT	–	–	−5.29	−4.08	−2.87	2.42	–
A	−3.3	0.178	−5.31	−4.07	−2.48	2.47	+2.0
Si_2-BC_2NNT	–	–	−5.25	−4.08	−2.91	2.34	–
B	−23.2	0.208	−5.06	−4.70	−4.25	0.71	−69.6

[a] Q is defined as the average of total Mulliken charge on the molecule

[b] The change of HOMO-LUMO gap of tube after H_2CO adsorption

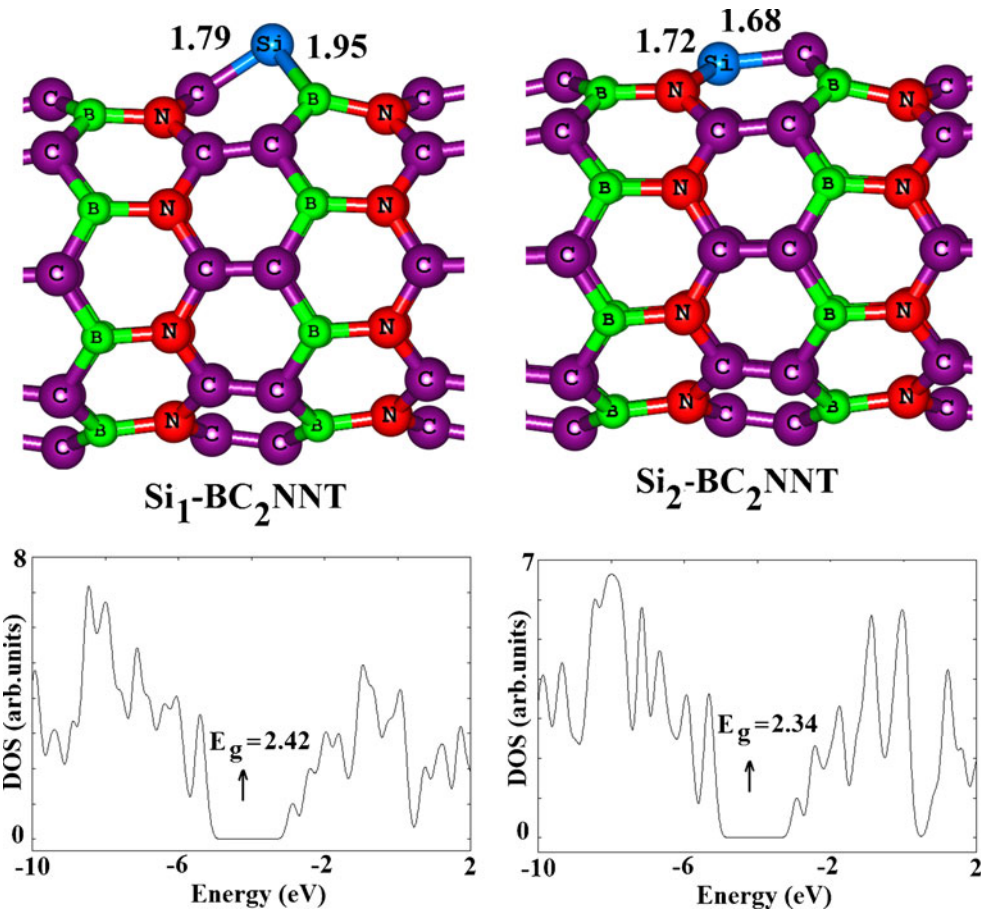

Fig. 3 Optimized structures of different Si-doped BC_2NNT and their density of states (DOS). Distances are in Å

H_2CO adsorption on Si-doped BC_2NNT

In the next step, Si-doped BC_2NNTs have been built in such a way that either a C_1 or a C_2 atom is substituted by a Si atom. When a C_1 was replaced by a Si (called Si_1-BC_2NNT, Fig. 3a), the E_{dop} was calculated to be +6.47 eV, but that was found to be about +3.76 eV for Si_2 doping process (called Si_2-BC_2NNT, Fig. 3b). These positive values indicate that both of the doping processes are endothermic and also suggest that the C_2 doping may be a more energetically favorable process than C_1 doping. Substituting the C atoms by the impurity of Si, geometric structure of the BC_2NNT is dramatically distorted, especially in the case of Si_1-BC_2NNT. In this structure, the Si impurity is projected out of the tube surface to reduce stress because of its larger size compared to the C atom. The calculated bond lengths are about 1.79 and 1.95 Å for the Si_1–C_2 and Si_1–B bonds, being much longer than the corresponding C_1-C_2 bonds in the pristine tube (Fig. 3a). Also, the B–Si_1–B angle in the doped tube is about 90° which is smaller than B–C_2–B in the pristine one (113°). NBO analysis suggests that it can be attributed to the change of doped atom hybridization from sp^2 to nearly sp^3. Calculated DOSs for both of the Si-doped BC_2NNTs are shown in Fig. 3, indicating that their E_g values are reduced to 2.42 and 2.34 eV compared to the pristine BC_2NNT. The DOS plots clearly show that the Si-doped BC_2NNTs are still semiconductor with a defect-related gap state.

Subsequently, we have explored H_2CO adsorption on both Si-doped tubes by locating the molecule above the Si atom with different initial orientations including H, C, or O atom of the molecule being close to the Si atom. We identified one distinct adsorptive configuration of H_2CO for each Si-doped BC_2NNT, namely **A** and **B**, as shown in Fig. 4. In both of these configurations, H_2CO molecule was located on the top of the doped Si atom from its oxygen head. The adsorption behavior of H_2CO on the Si-doped tubes is significantly different from that on the pristine BC_2NNT. Configuration **B** gives rise to an E_{ad} of −23.2 kcal mol^{-1}, which is more negative than the E_{ad} values for configuration **A** (−3.3 kcal mol^{-1}). From the above results, it is clear that the reactivity of

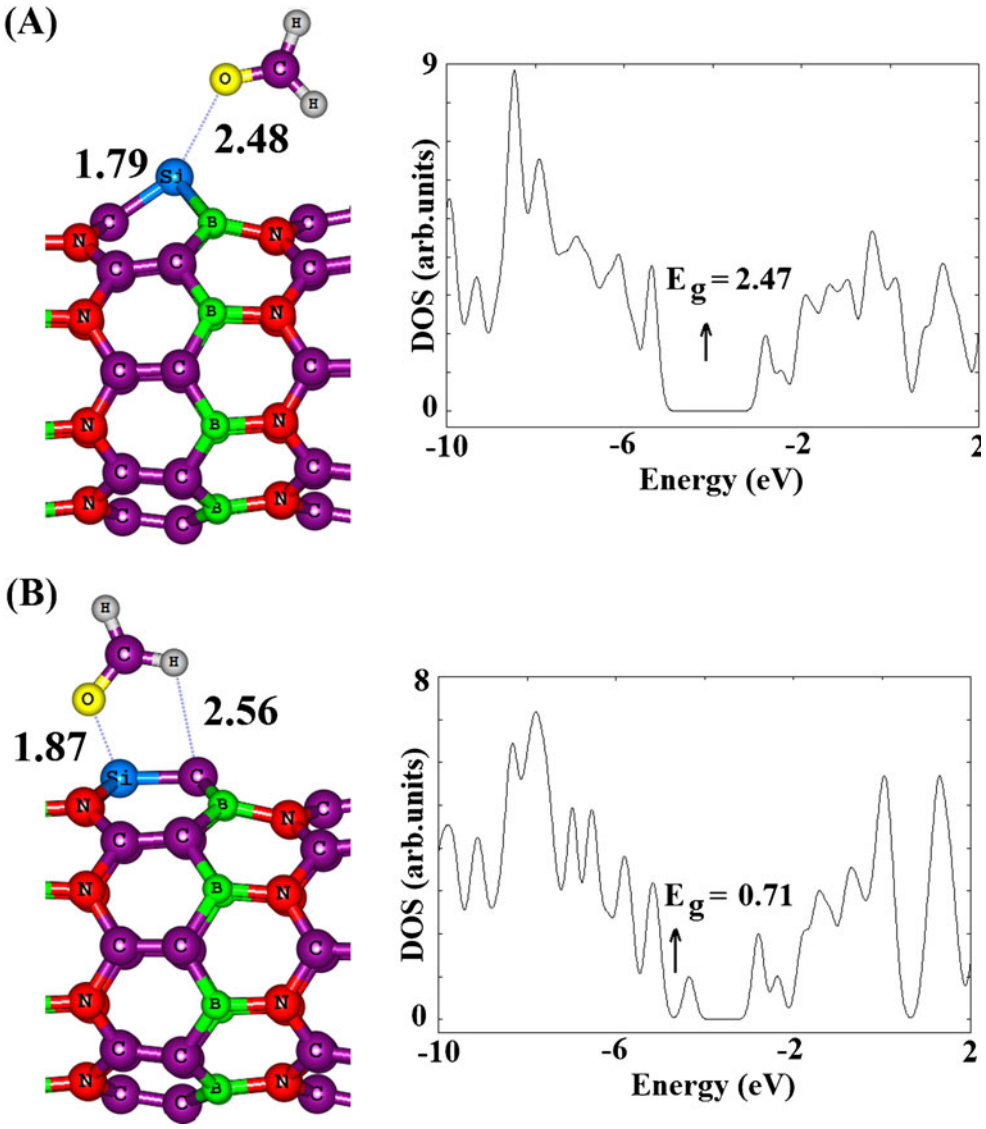

Fig. 4 Models for two stable adsorption states for a H_2CO molecule on the different Si-doped BC_2NNT and their density of states (DOS). Distances are in Å

the BC_2NNT toward the H_2CO molecule presents dramatic changes before and after the doping with the Si atom. In the doped BC_2NNT, the Si impurity Si_1 or Si_2 plays a crucial role in capturing the H_2CO molecule. In Table 1, we have summarized the results for E_{ad}, charge transfer, and E_g for H_2CO adsorption on the Si-doped BC_2NNTs.

In configuration **A** (Fig. 4), the oxygen atom of H_2CO molecule is collated on the top of the impurity Si_1 atom with the bond length of 2.48 Å. After the adsorption process, the length of Si_1-C_2 and Si_1-B bonds attached to molecule is changed to 1.78 and 1.93 Å, respectively. Calculated DOS plot (Fig. 4a) shows that the H_2CO adsorption through configuration **A** has no sensible effect on the electronic properties of the BC_2NNT, so that the E_g of the tube has a negligible change from 2.42 to 2.47 eV. In the most stable configuration (**B**, Fig. 4), a net charge of 0.208 *e* was transferred from the molecule to the tube and corresponding bond lengths of Si_2-C_1 and Si_2-N are 1.71 and 1.74 Å, respectively. These data indicate that the H_2CO molecule undergoes strong chemisorption on the Si_2-BC_2NNT. As shown in Fig. 4b, the distances between the O atom of H_2CO, and the Si_2 atom of the tube is 1.87 Å.

Unlike configuration **A**, the DOS plot of configuration **B** shows that the electronic properties of the nanotube are very sensitive to the H_2CO adsorption. By referring to Fig. 4b, the DOS near the conduction level has a distinct change compared to that of the doped tube, but valence level almost remains constant. The E_g was also decreased from 2.34 to

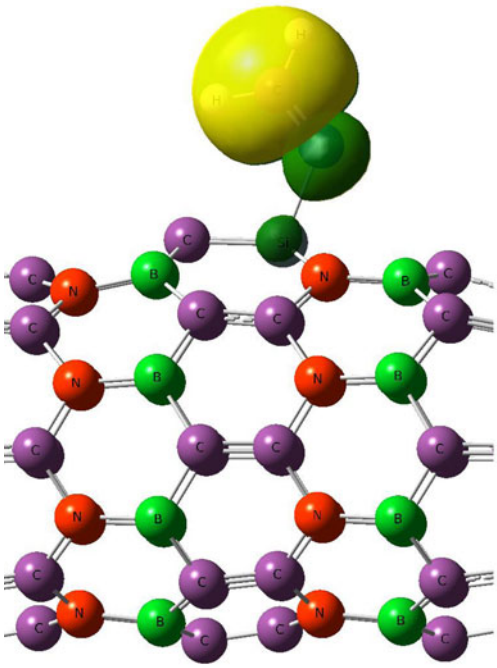

Fig. 5 The LUMO profile of H_2CO/Si_2-BC_2NNT

0.71 eV after the adsorption of H_2CO molecule. Calculated profile of LUMO for configuration **B** (Fig. 5) demonstrates that the LUMO has shifted on the adsorbed formaldehyde, while the HOMO has remained on the tube surface. It is well known that the E_g (or band gap in bulk materials) is a major factor determining the electrical conductivity of a material and there is a classic relation between them as follows [37]:

$$\sigma \propto \exp\left(\frac{-E_g}{2kT}\right) \tag{2}$$

where σ is the electrical conductivity and k is the Boltzmann's constant. According to the equation, smaller E_g at a given temperature leads to larger electrical conductivity.

Table 1 shows that the E_g of Si-doped BC_2NNT (configuration **B**) decreases by about 69.6 % after H_2CO adsorption. This will increase the conductivity of the tube according to Eq. 2. Compared with the pristine BC_2NNT, the Si_2-BC_2NNT may have H_2CO detection ability because of its suitable adsorption energy and conductivity change which may be converted to electrical signals. So we believe that Si doping process may be a strategy for improving the sensitivity of BC_2NNT to H_2CO, which cannot be trapped and detected by the pristine BC_2NNT.

Table 2 Calculated adsorption energy of a H_2CO (E_{ad}, kcal mol^{-1}), HOMO energies (E_{HOMO}), LUMO energies (E_{LUMO}), Fermi level energies and HOMO-LUMO energy gap (E_g) for pristine and Si doped BC_2NNT at M06/6-31G(d). Energies are in eV

System	E_{ad}	[a]Q_T (e)	E_{HOMO}	E_F	E_{LUMO}	E_g	[b]ΔE_g(%)
BC_2NNT	–	–	−5.75	−4.21	−2.68	3.07	–
H_2CO/BC_2NNT	−1.8	0.053	−5.71	−4.19	−2.67	3.04	−1.0
Si_1-BC_2NNT	–	–	−5.63	−4.17	−2.71	2.92	–
A	−4.2	0.078	−5.65	−4.16	−2.68	2.97	+1.7
Si_2-BC_2NNT	–	–	−5.59	−4.17	−2.76	2.83	–
B	−25.2	0.237	−5.38	−4.79	−4.20	1.18	−58.3

[a] Q is defined as the average of total Mulliken charge on the molecule

[b] The change of HOMO-LUMO gap of tube after H_2CO adsorption

Table 3 Calculated adsorption energy of a H_2CO (E_{ad}, kcal mol^{-1}), HOMO energies (E_{HOMO}), LUMO energies (E_{LUMO}), Fermi level energies and HOMO-LUMO energy gap (E_g) for pristine and Si doped BC_2NNT at B3LYP/6-311++G(d,p). Energies are in eV

System	E_{ad}	[a]Q_T (e)	E_{HOMO}	E_F	E_{LUMO}	E_g	[b]ΔE_g(%)
BC_2NNT	–	–	−5.67	−4.37	−3.07	2.60	–
H_2CO/BC_2NNT	−1.01	0.045	−5.50	−4.25	−3.00	2.50	−3.8
Si_1-BC_2NNT	–	–	−5.54	−4.31	−3.09	2.45	–
A	−3.5	0.084	−5.56	−4.32	−3.08	2.48	+1.2
Si_2-BC_2NNT	–	–	−5.51	−4.32	−3.13	2.38	–
B	−24.1	0.174	−5.32	−4.94	−4.57	0.75	−68.5

[a] Q is defined as the average of total Mulliken charge on the molecule

[b] The change of HOMO-LUMO gap of tube after H_2CO adsorption

As mentioned in H2CO adsorption on pristine BC2NNT, Zhang et al. [35] by using the generalized-gradient approximation functional with the Perdew-Wang functional (PW91) have shown that the E_{ad} of H_2CO on the BNNT dramatically increased from 1.2 to 42.0 kcal mol^{-1} after Si doping. They found that Si doping can also improve the sensitivity of BNNT toward H_2CO. Unlike BNNT, in which both forms of Si_N-BNNT and Si_B-BNNT can detect H_2CO, we have shown that just one form of Si-doped BC_2NNT (Si_2-BC_2NNT) is sensitive toward the target molecule.

Finally, we have explored the effect of DFT functional, basis set and tube length on the obtained results. The dispersion term to the total energy may give a non-negligible contribution, especially in the calculation of the H_2CO physisorption. Therefore, we have repeated all of the energy calculations, using dispersion corrected functional M06 [38] with the same basis set. The results were summarized in Table 2, showing that the E_{ad} values of M06 are somewhat more negative than those of the B3LYP, especially in the two cases of weak interactions (H_2CO/BC_2NNT and **A**). It may be due to the fact that the M06 includes dispersion interactions. As shown in Table 2, the energies of HOMO, LUMO and Fermi level slightly changed by changing the functional. It was found that the E_g values depend on the type of functional method.

As seen in Table 2, although the calculated values of E_g for the studied systems using M06/6-31G(d) are somewhat larger than the results of B3LYP, both functionals indicate that the E_g of Si_2-BC_2NNT significantly changes after formaldehyde adsorption (configuration **B**). Also, the results of a larger basis set (6-311++G(d,p)) in Table 3 show that the effect of basis set is less than that of functional. In addition, we have repeated the calculations on a longer BC_2NNT constructed of 40 B, 40 N and 80 C atoms where its optimized length with the B3LYP functional and 6-31G(d) basis set is about 20.11 Å. The results indicated that the change in length has insignificant influence on the energy values. The calculated E_g for this tube is about 2.54 eV which is slightly smaller than that of the shorter tube (2.57 eV). Overall, in contrast to the used method and basis set, the effect of tube length may be negligible on the obtained results.

Conclusions

The geometric structures and electronic properties of the pristine and different Si-doped BC_2NNTs were explored in the presence and absence of an H_2CO molecule using DFT calculations. It was found that the H_2CO molecule weakly interacts with the pristine BC_2NNT, but it presents much higher reactivity toward the Si-doped BC_2NNT. E_{ad} on the pristine tube is about −0.8 kcal mol^{-1}, while it is about −3.3 to −23.2 kcal mol^{-1} on the doped tubes at B3LYP/6-31G(d). Based on DOS analysis, it was suggested that Si-doped BC_2NNTs may be used as a H_2CO gas sensor. BC_2NNT in which a C_2 atom is substituted by a Si one is more favorable for H_2CO adsorption.

References

1. Dinadayalane TC, Murray JS, Concha MC, Politzer P, Leszczynski J (2010) J Chem Theory Comput 6:1351–1357
2. Politzer P, Murray J, Lane P, Concha M, Jin P, Peralta-Inga Z (2006) J Mol Model 12:528
3. Chu H, Wei L, Cui R, Wang J, Li Y (2010) Coord Chem Rev 254:1117–1134
4. Beheshtian J, Peyghan AA, Bagheri Z (2012) Phys E 44:1963–1968
5. Beheshtian J, Ahmadi Peyghan A, Bagheri Z (2012) J Mol Model 19:255–261
6. Beheshtian J, Peyghan AA, Bagheri Z (2012) Monatsh Chem/Chem Mon 143:1623–1626
7. Li Z, Jia Z, Luan Y, Mu T (2008) Curr Opinion Solid State Mater Sci 12:1–8
8. Lim SH, Luo J, Ji W, Lin J (2007) Catal Today 120:346–350
9. Blase X, Charlier JC, De Vita A, Car R (1997) Appl Phys Lett 70:197–199
10. Baei MT, Peyghan AA, Bagheri Z (2013) Solid State Commun 159:8–12
11. Ahmadi Peyghan A, Hadipour N, Bagheri Z (2013) J Phys Chem C 117:2427–2432
12. Rossato J, Baierle RJ, Orellana W (2007) Phys Rev B 75:235401–235407
13. Sen R, Satishkumar BC, Govindaraj A, Harikumar KR, Gargi R, Zhang JP, Cheetham AK, Rao CNR (1998) Chem Phys Lett 287:671–676
14. Redlich P, Loeffler J, Ajayan PM, Bill J, Aldinger F, Rühle M (1996) Chem Phys Lett 260:465–470
15. Bai XD, Guo JD, Yu J, Wang EG, Yuan J, Zhou WZ (2000) Appl Phys Lett 76:2624–2626
16. Raidongia K, Jagadeesan D, Upadhyay-Kahaly M, Waghmare UV, Pati SK, Eswaramoorthy M, Rao CNR (2008) J Mater Chem 18:83–90
17. Korpan YI, Gonchar MV, Sibirny AA, Martelet C, El'skaya AV, Gibson TD, Soldatkin AP (2000) Biosens Bioelectron 15:77–83
18. Zhou KW, Ji XL, Zhang N, Zhang XR (2006) Sensors Actuators B 119:392–397
19. Feng L, Liu YJ, Zhou XD, Hu JM (2005) J Colloid Interface Sci 284:378–382
20. Herschkovitz Y, Eshkenazi I, Campbell CE, Rishpon J (2000) J Electroanal Chem 491:182–187
21. Dai J, Giannozzi P, Yuan J (2009) Surf Sci 603:3234–3238
22. Leenaerts O, Partoens B, Peeters FM (2008) Phys Rev B 77:125416–125421
23. Wehling TO, Noveselov KS, Morozov SV, Vdovin EE, Katsnelson MI, Geim AK, Lichtenstein AI (2008) Nano Lett 8:173–177
24. Dai J, Yuan J, Giannozzi P (2009) Appl Phys Lett 95:232105–232107
25. Carrillo I, Rangel E, Magaña LF (2009) Carbon 47:2752–2754
26. Becke AD (1988) Phys Rev A 38:3098–3100
27. Lee C, Yang W, Parr RG (1988) Phys Rev B 37:785–789
28. Schmidt MW, Baldridge KK, Boatz JA, Elbert ST, Gordon MS, Jensen JH, Koseki S, Matsunaga N, Nguyen KA, Su S (2004) J Comput Chem 14:1347–1363

29. Chen L, Xu C, Zhang XF, Zhou T (2009) Phys E 41:852–855
30. Beheshtian J, Bagheri Z, Kamfiroozi M, Ahmadi A (2012) J Mol Model 18:2653–2658
31. Beheshtian J, Peyghan AA, Bagheri Z (2012) Sensors Actuators B Chem 171–172:846–852
32. Beheshtian J, Soleymanabadi H, Kamfiroozi M, Ahmadi A (2012) J Mol Model 18:2343–2348
33. Boys SF, Bernardi F (1970) Mol Phys 19:553–566
34. Olmsted J, Williams GM (1997) Chemistry: the molecular science. WCB, Dubuque, IA
35. Wang R, Zhu R, Zhang D (2008) Chem Phys Lett 467:131–135
36. Wang X, Liew KM (2011) J Phys Chem C 115:10388–10393
37. Li S (2006) Semiconductor physical electronics, 2nd edn. Springer, Heidelberg
38. Zhao Y, Truhlar DG (2006) J Chem Phys 125:194101–194118